Electronic Supplementary Information

Constructing 2D/2D interfacial contact in ReS_2/TiO_2 via Ti-S bond for efficient charge transfer in photocatalytic hydrogen production

Yanan Wang[a], Rongrong Shi[a], Kai Song[a], Chunyang Liu[a] and Fang He*[, a]

[a]School of Materials Science and Engineering and Tianjin Key Laboratory of Composite and Functional Materials, Tianjin University, Tianjin, 300350, P.R. China.

*Corresponding Author. E-mail: fanghe@tju.edu.cn.

The gas reactions in chemical vapor deposition

In the experiment, NH_4ReO_4 decompose thermally into gaseous Re_2O_7 volatilizing according to following equation[1]:

$$2NH_4ReO_4\ (s) + (3/2)O_2\ (g) = Re_2O_7\ (g) + 4H_2O\ (g) + N_2\ (g) \quad (1)$$

Re_2O_7 obtained by thermal decomposition of NH_4ReO_4 may be further oxidized into ReO_4 or deoxidized into ReO_3, ReO_2 and even Re at high temperatures.

$$Re_2O_7\ (g) + (1/2)O_2\ (g) = 2ReO_4 \quad (2)$$

$$Re_2O_7\ (g) = 2ReO_3 + (1/2)O_2\ (g)\ (\text{bellow } 527\ ^\circ\text{C}) \quad (3)$$

$$Re_2O_7\ (g) = 2ReO_2 + (3/2)O_2\ (g)\ (\text{above } 527\ ^\circ\text{C}) \quad (4)$$

$$ReO_3\ (g) = 2ReO_2 + (1/2)O_2\ (g) \quad (5)$$

$$2ReO_2\ (g) = 2Re + 2O_2\ (g) \quad (6)$$

In the experiment, the above reaction cannot proceed completely. After kept for a certain period of time (10 min) at the temperature (700 ℃) of CVD, ReS_2 nanosheets were obtained by direct sulfidization of ReO_2[2, 3] and large amount of SO_2 are released[4]. Finally, ReS_2 nanosheets are deposited on the TiO_2 surface via Ti-S bond to form 2D/2D interfacial contact in ReS_2/TiO_2.

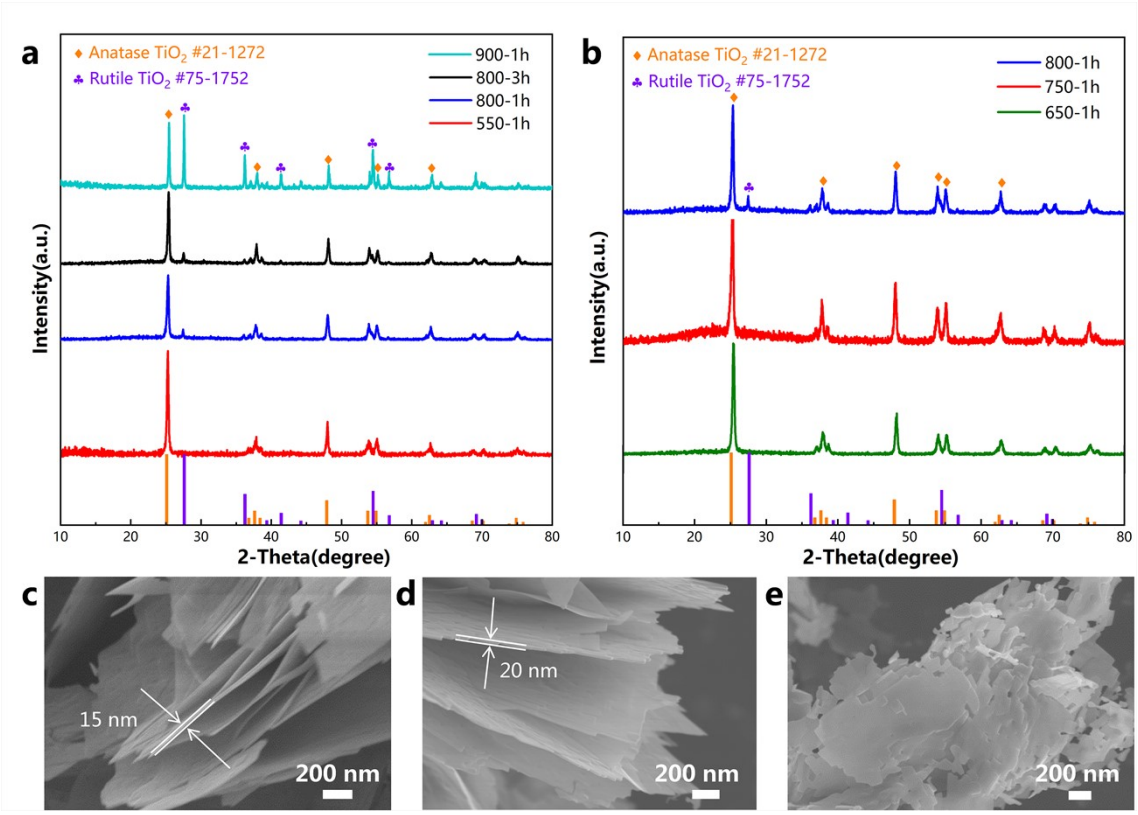

Figure S1 XRD patterns of TiO_2 calcined at different temperatures for 1 h (a, b) and calcined at 800 ℃ for 3h (black) in (a); SEM images of 550TiO_2 (c), 800TiO_2 (d) and 900TiO_2 (e).

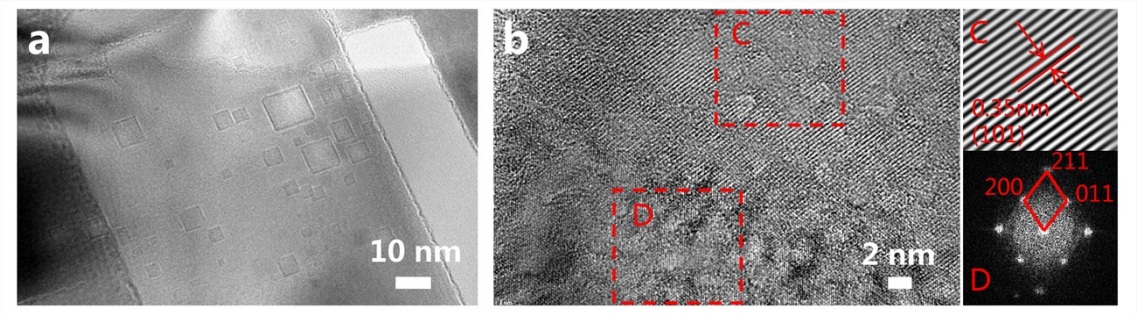

Figure S2 (a, b) TEM images of 800TiO_2, the inset C is the fringe spacing of the region C and D is the diffraction spots of the region D in Figure S2.

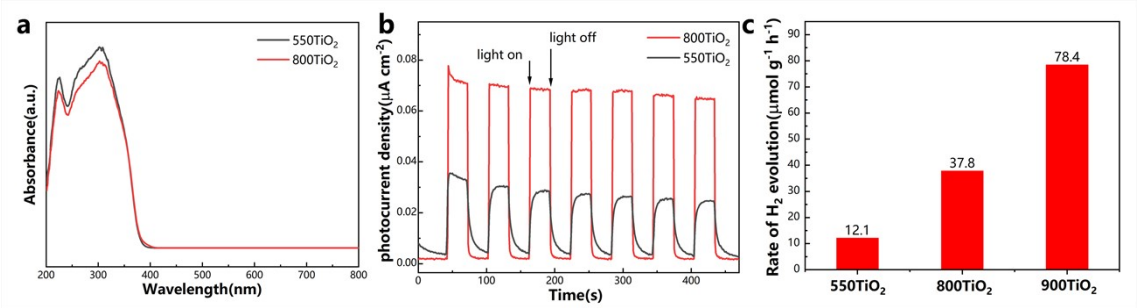

Figure S3 (a) UV-vis absorption spectra; (b) photocurrent density−time curves of $550TiO_2$ and $800TiO_2$ and (c) Comparison of the photocatalytic hydrogen production activities of TiO_2.

Ultraviolet−visible (UV−vis) spectra are employed to investigate the optical absorption of TiO_2. As shown in Figure S3a, $550TiO_2$ and $800TiO_2$ have similar optical absorption range, mainly light absorption in the UV region (≤400 nm). As observed in Figure S3b, the transient photocurrent responses of $550TiO_2$ and $800TiO_2$ are measured at a bias potential of 0.6 V under UV-vis irradiation. The two photo-electrodes displayed a mild photocurrent response in the dark. When the light turns on, $800TiO_2$ presents a higher photocurrent than single phase ($550TiO_2$), suggesting that the mixed phases TiO_2 has stronger photocurrent response and lower recombination efficiency of photo-generated charge carriers. Subsequently, the photocatalytic hydrogen production tests are carried out under UV-vis irradiation. As depicted in Figure S3c, the two mixed phases TiO_2 ($800TiO_2$ and $900TiO_2$) show a significant increase in the hydrogen evolution performance, compared with the anatase TiO_2 ($550TiO_2$).

Table S1 Observed Raman peaks (cm^{-1}) of TiO_2, ReS_2 and their corresponding assignments.

Anatase TiO_2		**Anatase TiO_2**			
Raman peak (cm^{-1})	**Assignment**	**Raman peak (cm^{-1})**	**Assignment**	**Raman peak (cm^{-1})**	**Assignment**
143.4	$E_{g(1)}$	**143.4**	B_{1g}	**148.7**	E_g
195.8	$E_{g(2)}$			**211.0**	A_g-like
396.3	$B_{g(1)}$			**305.2**	E_g-like
515.7	$A_{g(1)}$				
515.7	$B_{g(2)}$				
638.9	$E_{g(3)}$				

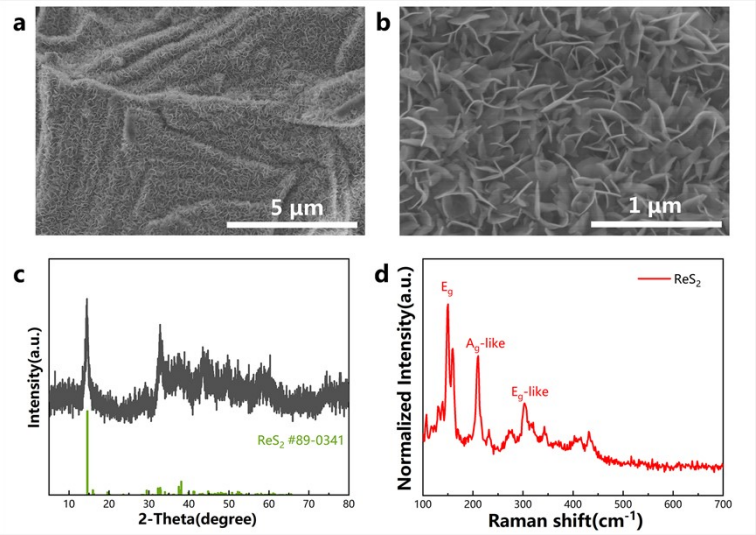

Figure S4 SEM images (a, b), XRD pattern (c) and Raman spectra (d) of ReS_2.

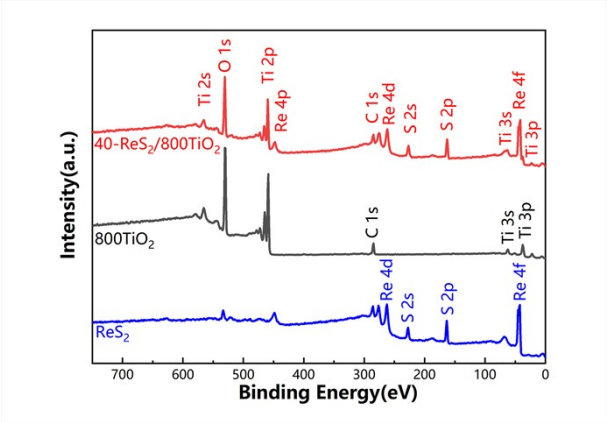

Figure S5 XPS survey spectra of ReS_2, $800TiO_2$ and 40-ReS_2/$800TiO_2$.

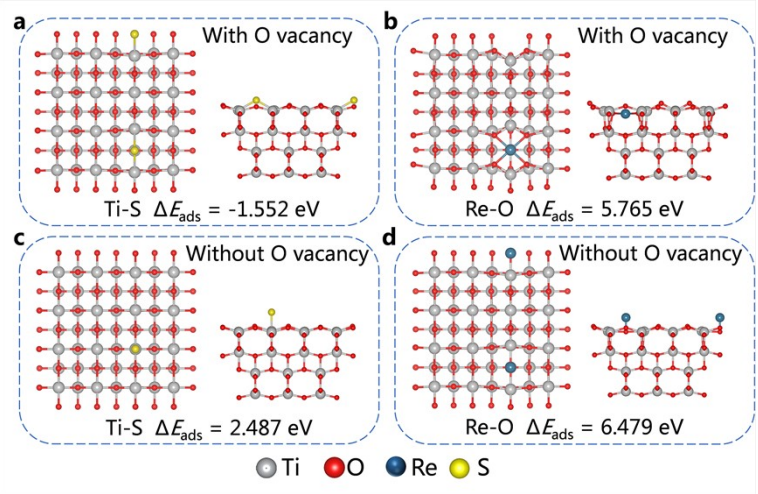

Figure S6 Four possible related structures accompanied by Ti-S and Re-O bonds and their corresponding adsorption energies. The top view on the left and the side view on the right. (a) one S atom adsorbed on the defective TiO_2 surface accompanied by Ti-S bond; (b) one Re atom adsorbed on the defective TiO_2 surface accompanied by Re-O bond; (c) one S atom adsorbed on the ideal TiO_2 surface accompanied by Ti-S bond; (d) one Re atom adsorbed on the ideal TiO_2 surface accompanied by Re-O bond.

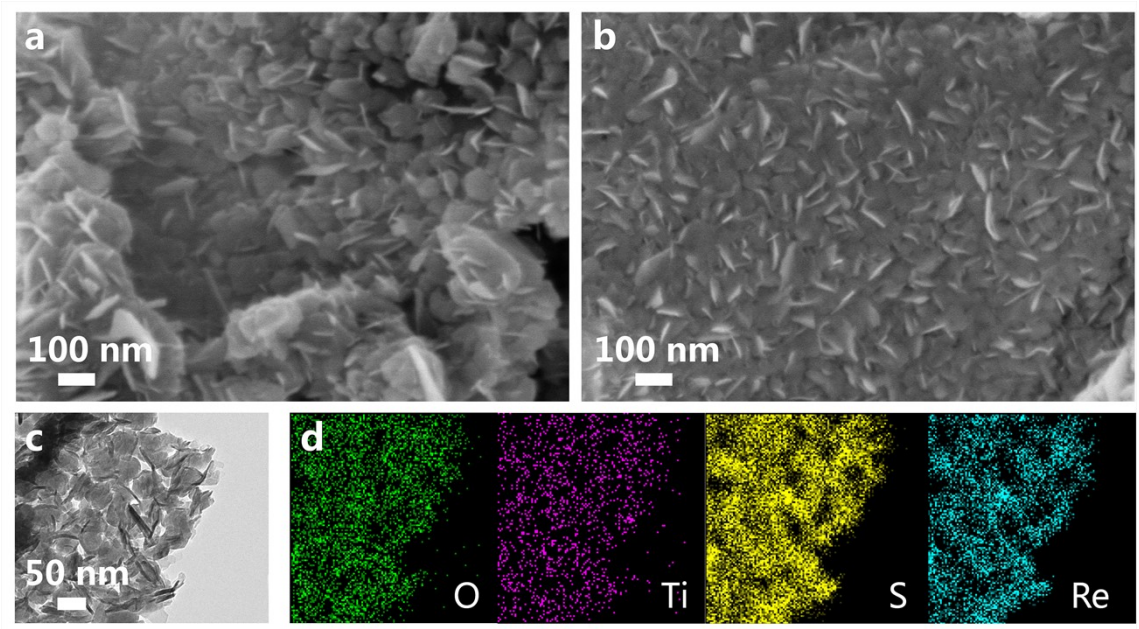

Figure S7 (a, b) SEM images, (c) TEM image and (d) element mapping images of ReS_2/H-TiO_2.

Synthesis of ReS_2/H-TiO_2:

To gain more O vacancies in the TiO_2 surface, 800TiO_2 is annealed in the tube furnace under H_2/Ar mixture gas (the gas flow ratio is 100/100 sccm) at 600 °C for 1h, denoted as H-TiO_2. ReS_2/H-TiO_2 composites were prepared by CVD at 700 °C for 10 min, which is the same weight ratio as 40-ReS_2/800TiO_2.

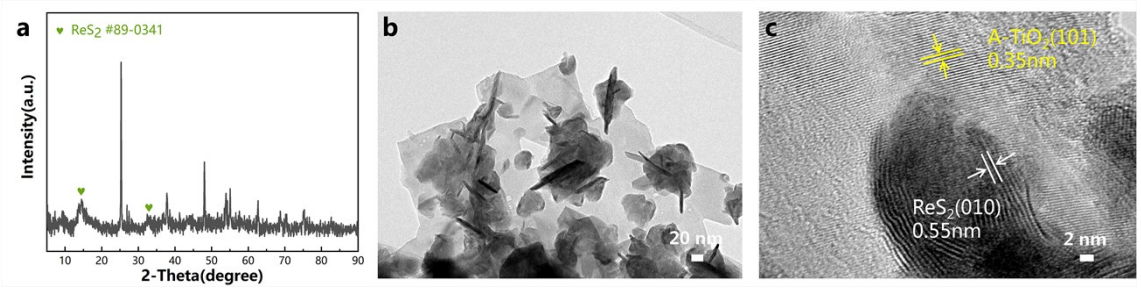

Figure S8 (a) XRD pattern, (b) TEM and (c) HRTEM images of 40-ReS_2/800TiO_2 after 9 h cycles.

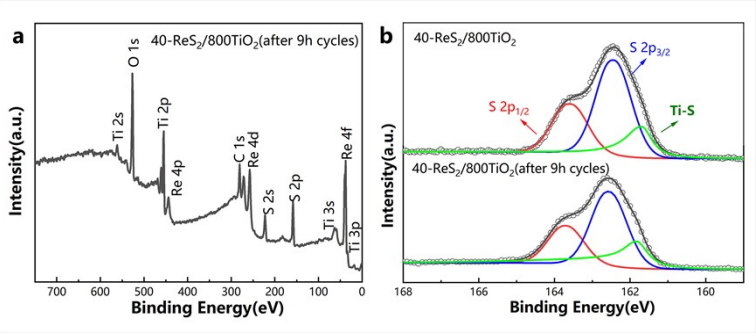

Figure S9 (a) XPS survey spectra of 40-ReS_2/800TiO_2 after 9 h cycles, (b) S 2p peaks of 40-ReS_2/800TiO_2 and 40-ReS_2/800TiO_2 after 9 h cycles.

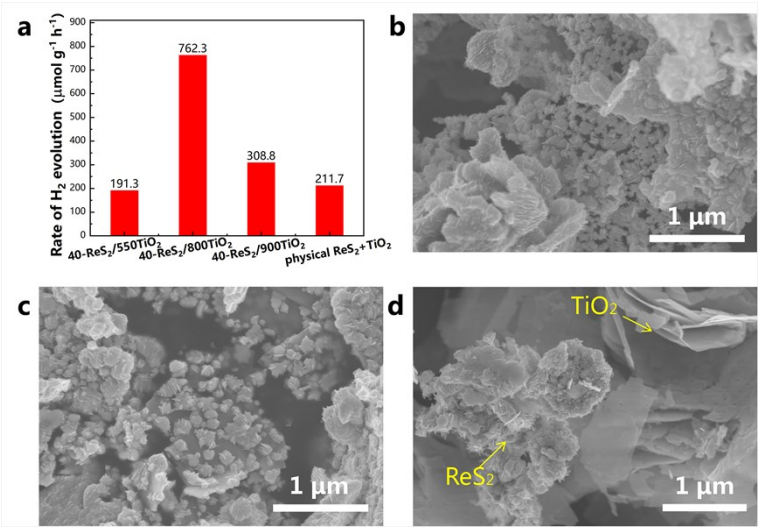

Figure S10 (a) Comparison of the photocatalytic hydrogen production activities of ReS_2/TiO_2; SEM images of $ReS_2/900TiO_2$ (b, c) and physical ReS_2+TiO_2 mixtures (d).

Figure S10b and c show the morphology of $ReS_2/900TiO_2$, which is very different from $ReS_2/800TiO_2$. Because the calcination temperature of $800TiO_2$ is higher than that of $900TiO_2$, there are more O vacancies on the surface of $900TiO_2$, which causes the increased loading of ReS_2 nanosheets, as shown in Figure S10b and c. Not only the loading of ReS_2 nanosheets increased, but also the agglomeration of ReS_2 nanosheets arose and ReS_2 nanosheets coated small-sized TiO_2. With the increase of the calcination temperature, the rutile ratio in TiO_2 increased (from 11% to 51%). It is possible that the state of rutile surface is not conducive to the growth of ReS_2, thus, ReS_2 is more likely to agglomerate to reduce the surface energy. To sum up, the increase of O vacancies and rutile ratio is the main reason for the agglomeration and the encapsulation of ReS_2 nanosheets, which also causes the photocatalytic hydrogen evolution performance of 40-$ReS_2/900TiO_2$ to be inferior to that of 40-$ReS_2/800TiO_2$.

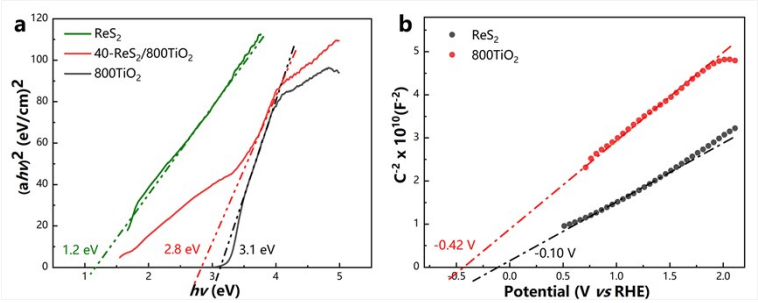

Figure S11 (a) the plots of $(\alpha h\nu)^2$ versus energy ($h\nu$) for the band gap energies of ReS_2, $800TiO_2$ and 40-ReS_2/$800TiO_2$; (b) Mott-Schottky plots of ReS_2 and $800TiO_2$.

In order to obtain the energy band diagrams of ReS_2/TiO_2, the optical absorption properties of $800TiO_2$, ReS_2 and 40-ReS_2/$800TiO_2$ are studied by UV-vis absorption spectroscopy (Figure 6d). Figure S11a presents that the band gap energies of $800TiO_2$, ReS_2, and 40-ReS_2/$800TiO_2$ are calculated as 3.1, 1.2 and 2.8 eV, respectively, according to the formula $\alpha h\nu = A(h\nu - E_g)^2$ (where α = absorbance, h = Planck's constant, and ν = frequency). Hence, the combination of cocatalyst ReS_2 improves the optical absorption of TiO_2, which induces more photo-generated carriers to participate in redox reaction. The Mott-Schottky (M-S) plots of $800TiO_2$ and ReS_2 shown in Figure S11b, the conduction band (CB) potential can be measured to be -0.42 and -0.1 V (vs RHE), corresponding to $800TiO_2$ and ReS_2, respectively. The band gap energy (E_g) of $800TiO_2$ and ReS_2 is calculated by the Tauc plot, thus, their valence band (VB) are calculated to be +2.68 and +1.10 V, respectively.

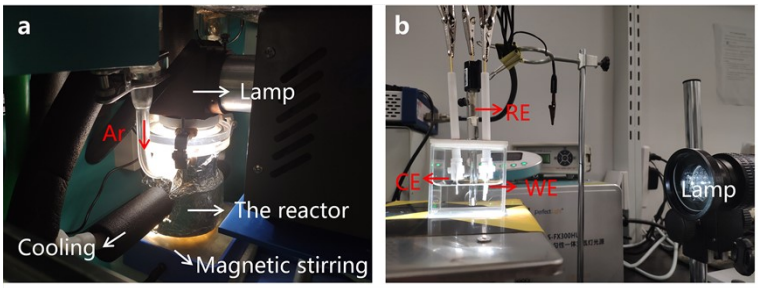

Figure S12 The reactors of photocatalytic hydrogen production test (a) and Photoelectrochemical Measurements (b).

References

1. M. Bai, Z.-h. Liu, L.-j. Zhou, Z.-y. Liu and C.-f. Zhang, *Transactions of Nonferrous Metals Society of China*, 2013, **23**, 538-542.
2. X.-h. Fan, Q. Deng, M. Gan and X.-l. Chen, *Transactions of Nonferrous Metals Society of China*, 2019, **29**, 840-848.
3. Q. Feng, M. Li, T. Wang, Y. Chen, X. Wang, X. Zhang, X. Li, Z. Yang, L. Feng, J. Zheng, H. Xu, T. Zhai and Y. Jiang, *Applied Catalysis B: Environmental*, 2020, **271**.
4. K. S. Coleman, J. Sloan, N. A. Hanson, G. Brown, G. P. Clancy, M. Terrones, H. Terrones and M. L. H. Green, *Journal of the American Chemical Society*, 2002, **124**, 11580-11581.